

# A Stabilizing Model Predictive Controller for Voltage Regulation of a DC/DC Boost Converter

Seok-Kyoon Kim, Chang Reung Park, Jung-Su Kim, and Young Il Lee

**Abstract**—This brief proposes a cascade voltage control strategy for the dc/dc converter utilizing a model predictive control (MPC) in the inner loop. The proposed MPC minimizes a cost function at each time step in the receding horizon manner and the corresponding optimal solution is obtained from a predefined function not relying on a numeric algorithm. It is shown that the MPC makes the capacitor voltage and the inductor current globally convergent in the presence of input constraints. State constraints also can be taken into account in the proposed MPC. Following the conventional cascade voltage control scheme, a Proportional-Integral (PI) controller is adopted in the outer loop. The experimental results show that the closed-loop performance is superior to the classical cascade PI control scheme.

**Index Terms**—Bilinear model, cascade control, dc/dc converter, global stability, input/state constraints, model predictive control (MPC).

## I. INTRODUCTION

WITH the advent of the smart grid and the renewable energy era, electronic power converters can be used extensively in various types of voltage regulation, such as solar photovoltaic systems, personal computers, computer peripherals, and adapters of consumer electronic devices to provide dc voltages by the switching action [2], [3]. Therefore, it is necessary to design the switching action logic such that the capacitor voltage closely follows its reference. By averaging the two different models corresponding to the cases in which a switch is ON and OFF, the power converter dynamics can be expressed as a bilinear model with a continuous control input. In addition, because the duty ratio for the switching action is treated as the control input, it is inherently constrained in a set determined by the minimum and maximum duty ratio.

Conventionally, because of the simplicity of the controller structure, the Proportional-Integral (PI) controllers [3]–[6] have been popular for stabilizing power converters under the cascade control strategy, which has the inner-loop current controller and the outer-loop voltage controller. However, the nonlinearity of the converter limits the closed-loop performance because the controllers were developed by using a linearized

model of the converter. In addition, they did not consider input constraints. In [7] and [8], a deadbeat controller and a predictive controller were devised for the inner loop to enhance the closed-loop performance. They linearized the nonlinear converter model and did not take input constraints into account. In order to handle the nonlinearity of the dc/dc converter, a sliding model controller [9]–[14] for the inner loop were presented without considering the physical input constraints.

Recently, there have been several nonlinear controllers [15]–[18], optimization-based linear feedback controllers [19]–[23] without use of the extra outer loop. Sliding mode controllers [15], [16] and feedback linearization controllers [17], [18] were developed with stability analysis. They also, however, did not consider input constraints and did not optimize the closed-loop performance. On the other hand, in [19]–[23], the stabilization of a nonlinear converter was attempted by using linear state feedback controllers. These controllers optimize a performance index under the linear matrix inequality constraints on the control input. However, they only ensure local asymptotic stability.

Model predictive control (MPC) is a receding horizon method in which the control input is calculated through an optimization procedure over finite numbers of future time steps at every time step. Consequently, physical constraints on the input and/or state variables can be handled effectively. Various MPC schemes have been developed to stabilize the power converters [24]–[30], taking the physical constraints into account. In [24], an MPC scheme was proposed without the use of pulsewidth modulation (PWM) techniques. With cost horizon 1, this MPC scheme optimizes a cost function including the error states on the finite set of all possible controls via the exhaustive search method. Although this control system is very simple to implement, the analysis of stability is not provided, and a high sampling frequency is required. The nonlinear MPCs [25]–[27] perform numerical online optimization with cost horizon 1 or 2, guaranteeing local asymptotic stability. In particular, the cost function includes the error states and the control input, and the corresponding solution was given by a numerical method, such as dual simplex linear programming, sequential quadratic programming, or the nonlinear extended predictive self-adaptive control algorithm [31]. On the other hand, explicit MPC schemes [28]–[30] were suggested using the multiparametric programming method proposed in [32] and [33]. Since the explicit MPC is given in the form of a lookup table, which is the analytical solution of the associated optimization problem, it allows to compute the MPC without any online optimization and makes it possible for the MPC to be used in electrical applications. However, since the explicit MPC is computed using the linearized or piecewise

Manuscript received August 27, 2013; revised November 16, 2013; accepted December 19, 2013. Manuscript received in final form December 19, 2013. This work was supported by the National Research Foundation of Korea through the Korean government under Grant 2010-0022103. Recommended by Associate Editor E. Kerrigan. (*Corresponding author: Y. I. Lee.*)

S.-K. Kim is with the Department of Electrical Engineering, Korea University, Seoul 136-701, Korea (e-mail: lotus45@korea.ac.kr).

C. R. Park, J.-S. Kim, and Y. I. Lee are with the Department of Electronics and Instrumentation Engineering, Seoul National University of Science and Technology, Seoul 139-743, Korea (e-mail: john316@seoultech.ac.kr; jungsu@seoultech.ac.kr; yilee@seoultech.ac.kr).

Color versions of one or more of the figures in this paper are available online at <http://ieeexplore.ieee.org>.

Digital Object Identifier 10.1109/TCST.2013.2296508

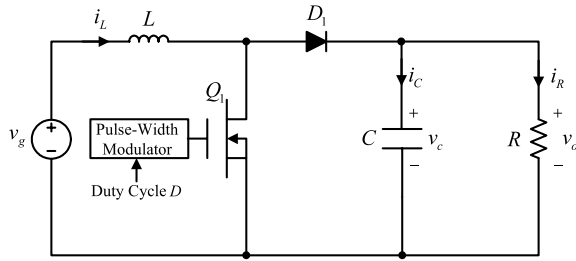


Fig. 1. Boost dc/dc converter.

affine models [28]–[30], [34], the explicit MPC may not work properly if there are model or parameters uncertainties. Note that these uncertainties are inevitable in practice and that, in particular, parameters variations can be severe in power converter models because of uncertainties in circuit elements. Hence, in order to control power converters modeled as bilinear systems, it would be nice to devise a tracking MPC scheme, which can be computed without any demanding online computation and provides a zero steady-state error systematically even in presence of parameter variations.

Under the classical cascade voltage control strategy, this brief proposes another type of MPC for the inner-loop current controller. The proposed MPC optimizes the cost function comprising the sum of the error states and deviation of the control based on the nonlinear converter model and the corresponding optimal solution is given explicitly without any online numerical optimization. It is proven that the capacitor voltage and the inductor current globally converge to their references in the presence of input constraints. In addition, it is seen that state constraints can be taken into account by the proposed MPC. Following the conventional cascade voltage control strategy, a PI controller is utilized in the outer loop. It is experimentally demonstrated that the proposed MPC provides better closed-loop performance and robustness than the classical cascade PI control scheme.

## II. DC/DC BOOST CONVERTER MODEL

In this brief, a dc/dc boost converter is analyzed. The circuit topology is shown in [35, Fig. 1].

Here, the PWM of the switching action is considered, i.e., if the duty ratio is  $D \in [0, 1]$ , the switch turns on for a period of  $DT$  and turns off for a period of  $(1 - D)T$ , where  $T$  is the PWM period. Therefore, the averaged model is obtained as follows:

$$\begin{aligned} \dot{\mathbf{x}}(t) = & (u(t)A_{c,1} + (1 - u(t))A_{c,2})\mathbf{x}(t) \\ & + (u(t)B_{c,1} + (1 - u(t))B_{c,2})\mathbf{v} \end{aligned} \quad (1)$$

where  $u(t) := D \in [D_{\min}, D_{\max}]$

$$\mathbf{x}(t) := \begin{bmatrix} i_L(t) \\ v_c(t) \end{bmatrix}^T, \quad \mathbf{v} := \begin{bmatrix} v_g \\ v_D \end{bmatrix}$$

$$A_{c,1} := \begin{bmatrix} -R_{\text{ON}}/L & 0 \\ 0 & -1/RC \end{bmatrix}$$

$$A_{c,2} := \begin{bmatrix} 0 & -1/L \\ 1/C & -1/RC \end{bmatrix}$$

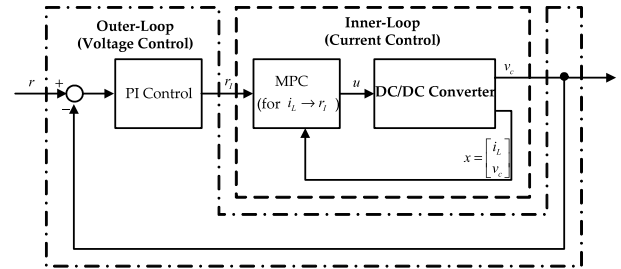


Fig. 2. Entire control system.

$$B_{c,1} := \begin{bmatrix} 1/L & 0 \\ 0 & 0 \end{bmatrix}, \quad B_{c,2} := \begin{bmatrix} 1/L & -1/L \\ 0 & 0 \end{bmatrix}$$

where  $R$  represents a load resistance,  $R_{\text{ON}}$  is the ON-resistance of MOSFET  $Q_1$ , and  $v_D$  is the diode voltage. Note that  $D_{\min}$  and  $D_{\max}$  could be 0 and 1, respectively. However, these constants can be utilized as design parameters to adjust the conservativeness of the stability condition in later derivations. For simplicity, define

$$B_c := (B_{c,1} - B_{c,2})\mathbf{v}, \quad G_c := A_{c,1} - A_{c,2}.$$

Then, the state equation (1) can be compactly written as

$$\dot{\mathbf{x}}(t) = A_{c,2}\mathbf{x}(t) + (B_c + G_c\mathbf{x}(t))u(t) + B_{c,2}\mathbf{v}. \quad (2)$$

A discrete-time version of the continuous-time system (2) can be obtained via the forward Euler approximation to yield

$$\mathbf{x}(k+1) = A_2\mathbf{x}(k) + (B + G\mathbf{x}(k))u(k) + B_2\mathbf{v} \quad (3)$$

where

$$A_2 := hA_{c,2} + I, \quad B := hB_c, \quad G := hG_c, \quad B_2 := hB_{c,2} \quad (4)$$

and  $h$  is the sampling period. Many types of dc/dc converters, such as buck, boost, buck-boost, and flyback (including multiswitch converters) can be described by a bilinear state equation, such as (1) [19], [35], [36]. For the rest of this brief, we devise an MPC for a boost converter. However, this controller design methodology can also be used for other dc/dc converters. Based on this discrete-time model and with a given current reference  $r_I$ , an MPC strategy is designed to drive the inductor current to its reference  $r_I$  in the presence of input constraints.

## III. STABILIZING MPC DESIGN FOR INNER LOOP

In this section, an MPC scheme, which requires a very simple online optimization procedure, is presented for the inner-loop current controller in the cascade control system (Fig. 2). The objective of the inner-loop current controller is to track its current reference signal  $r_I$ . Thus, an MPC scheme is designed for the inner loop so that

$$\lim_{k \rightarrow \infty} i_L(k) = r_I. \quad (5)$$

First, a steady-state condition is derived in Section III-A. In Section III-B, we consider a cost function containing terms for the error states and deviation of the input. An online solution is derived in the presence of input constraints without any use of numerical methods. Section III-C proves that the MPC makes the capacitor voltage and inductor current globally convergent. Section III-D presents an MPC solution in the presence of state constraints.

### A. Steady-State Condition

In this section, a steady-state condition for the inner-loop controller is presented for a given inductor current reference,  $r_I$ . For this purpose, let  $\mathbf{x}^0 := [x_1^0 \ x_2^0]^T$  and  $u^0$  be the steady state of state  $\mathbf{x}(k)$  and input  $u(k)$  satisfying

$$\mathbf{x}^0 = A_2 \mathbf{x}^0 + (B + G \mathbf{x}^0) u^0 + B_2 \mathbf{v} \quad (6)$$

$$x_1^0 = r_I, \quad u^0 \in [D_{\min}, D_{\max}] \quad (7)$$

where  $x_1^0$  is the steady state of the inductor current. Then, inserting  $x_1^0 = r_I$  into (6) and through algebraic calculations, steady state  $\mathbf{x}^0$  and corresponding steady-state control  $u^0$  are calculated as

$$\mathbf{x}^0(r) = \begin{bmatrix} x_1^0(r) \\ x_2^0(r) \end{bmatrix} = \begin{bmatrix} r_I \\ \frac{-a_1(r) \pm \sqrt{a_1(r)^2 - 4a_0(r)a_2}}{2a_2} \end{bmatrix} \quad (8)$$

$$u^0(r) = \frac{(1 - a_{2,1})r_I - a_{2,2}x_2^0(r) - b_{2,1}v_g - b_{2,2}v_D}{b_1 + g_1r_I + g_2x_2^0(r)} \quad (9)$$

where

$$a_0(r) := -(a_{2,3}r_I + b_{2,3}v_g + b_{2,4}v_D)(b_1 + g_1r_I) \\ - ((1 - a_{2,1})r_I - b_{2,1}v_g - b_{2,2}v_D)(b_2 + g_3r_I)$$

$$a_1(r) := (b_1 + g_1r_I)(1 - a_{2,4}) \\ - (a_{2,3}r_I + b_{2,3}v_g + b_{2,4}v_D)g_2 + a_{2,2}(b_2 + g_3r_I) \\ - ((1 - a_{2,1})r_I - b_{2,1}v_g - b_{2,2}v_D)g_4$$

$$a_2 := ((1 - a_{2,4})g_2 + a_{2,2}g_4)$$

$a_{2,i}$ ,  $b_j$ ,  $b_{2,i}$ ,  $g_i$ ,  $i = 1, 2, 3, 4$ ,  $j = 1, 2$ , are the elements of matrices  $A_2$ ,  $B$ ,  $B_2$ , and  $G$ . Hence, it turns out that inductor current reference  $r_I$  must be selected so that the capacitor voltage steady state,  $x_2^0(r)$ , is real and the steady-state control,  $u^0(r)$ , in (9) belongs to set  $[D_{\min}, D_{\max}]$  in order to make the control objective meaningful. For the rest of this brief, the inductor current reference  $r_I$  is called admissible when it meets these two conditions.

In view of (8), there can be two possible solutions for the steady state of the inductor current  $x_2^0(r)$  for a given reference,  $r_I$ . When there are two solutions, one of the two is chosen such that the corresponding steady-state control,  $u^0(r)$ , belongs to set  $[D_{\min}, D_{\max}]$ .

### B. MPC Design

This section presents an MPC method for a discrete-time system (3). For this purpose, define the error state as  $\mathbf{e}_x(k) := \mathbf{x}(k) - \mathbf{x}^0(r_I)$ . Then, subtracting (6) from (3), the following error dynamics is obtained:

$$\mathbf{e}_x(k+1) = A_2 \mathbf{e}_x(k) + G \mathbf{e}_x(k) u(k) + T \tilde{u}(k) \quad (10)$$

where  $T := B + G \mathbf{x}^0(r_I)$  and  $\tilde{u}(k) := u(k) - u^0(r_I)$ . We construct the cost function in terms of the error state and deviation of the input from  $u^0(r)$   $\tilde{u}(k) := u(k) - u^0(r_I)$  as follows:

$$J(\mathbf{e}_x(k), u(k)) := \mathbf{e}_x^T(k+1) P_c \mathbf{e}_x(k+1) + \rho \tilde{u}^2(k) \quad (11)$$

where  $P_c = P_c^T > 0$  and  $\rho \geq 0$  are the design parameters. Now consider the following optimization problem:

$$\min_{u(k) \in [D_{\min}, D_{\max}]} J(\mathbf{e}_x(k), u(k)) \quad \forall k \geq 0. \quad (12)$$

It is observed that the optimizer of this optimization problem at time  $k$  minimizes the one-step future error state as well as deviation of the input while satisfying the input constraint. In order to derive the optimizer of the optimization problem (12), rewrite the cost function (11) as

$$J(\mathbf{e}_x(k), u(k)) = c_2(\mathbf{e}_x(k)) u(k)^2 + c_1(\mathbf{e}_x(k)) u(k) \\ + c_0(\mathbf{e}_x(k)) + \rho \tilde{u}^2(k) \quad (13)$$

where  $c_i(\mathbf{e}_x(k))$ ,  $i = 0, 1, 2$ , are coefficients of  $u(k)$  given by

$$c_0(\mathbf{e}_x(k)) := (A_2 \mathbf{e}_x(k) - T u^0(r_I))^T P_c (A_2 \mathbf{e}_x(k) - T u^0(r_I)) \\ c_1(\mathbf{e}_x(k)) := 2(T + G \mathbf{e}_x(k))^T P_c (A_2 \mathbf{e}_x(k) - T u^0(r_I)) \\ c_2(\mathbf{e}_x(k)) := (T + G \mathbf{e}_x(k))^T P_c (T + G \mathbf{e}_x(k)).$$

Let  $u_{uc}^*(\mathbf{e}_x(k))$  be the unconstrained solution of the optimization problem (12). Then, the solution of (13) can be obtained by solving  $(\partial J(\mathbf{e}_x(k), u(k)))/(\partial u(k)) = 0$

$$u_{uc}^*(\mathbf{e}_x(k)) = \frac{-c_1(\mathbf{e}_x(k)) + 2\rho u^0(r_I)}{2(c_2(\mathbf{e}_x(k)) + \rho)}. \quad (14)$$

Hence, it is obvious that optimizer  $u^*(\mathbf{e}_x(k))$  of the constrained problem (12) is the same as  $u_{uc}^*(\mathbf{e}_x(k))$  if  $D_{\min} \leq u_{uc}^*(\mathbf{e}_x(k)) \leq D_{\max}$ . On the contrary, if  $u_{uc}^*(\mathbf{e}_x(k)) < D_{\min}$ , the constrained optimizer  $u^*(\mathbf{e}_x(k))$  is  $D_{\min}$ , and if  $u_{uc}^*(\mathbf{e}_x(k)) > D_{\max}$ , the constrained optimizer  $u^*(\mathbf{e}_x(k))$  is  $D_{\max}$ . In conclusion, the MPC algorithm  $u^*(\mathbf{e}_x(k))$  is established by

$$u^*(\mathbf{e}_x(k)) = \begin{cases} u_{uc}^*(\mathbf{e}_x(k)) & \text{(of (14)),} \\ \text{if } D_{\min} \leq u_{uc}^*(\mathbf{e}_x(k)) \leq D_{\max} \\ D_{\min}, & \text{if } u_{uc}^*(\mathbf{e}_x(k)) < D_{\min} \\ D_{\max}, & \text{if } u_{uc}^*(\mathbf{e}_x(k)) > D_{\max}. \end{cases} \quad (15)$$

### C. Stability Analysis

In this section, it will be shown that the MPC given as (15) makes the error state globally convergent provided that the matrix  $P_c$  of the cost function (11) is properly chosen. Here, we assume that the current reference  $r_I$  is admissible and consider the cost function (11) at time  $k$ . The closed-loop stability can be obtained in two steps. First, the monotonicity of  $J(\mathbf{e}_x(k), u(k))$  will be checked under the use of the steady-state input, i.e.,  $u(k) = u^0(r_I)$ . Then, the monotonicity of  $J(\mathbf{e}_x(k), u(k))$  under the use of the MPC (15) can be obtained in comparison with the case of  $u(k) = u^0(r_I)$ . To this end, for a given error state  $\mathbf{e}_x(k)$  generated by  $\mathbf{e}_x(k-1)$  and  $u(k-1)$ , let  $\mathbf{e}_x^0(k+1)$  and  $\mathbf{e}_x^*(k+1)$  represent the error states in the next time step obtained by the use of the steady-state input  $u(k) = u^0(r_I)$  and the MPC  $u(k) = u^*(\mathbf{e}_x(k))$ , respectively. With these notations, write  $J(\mathbf{e}_x(k), u^0(r_I))$  as

$$J(\mathbf{e}_x(k), u^0(r_I)) = \mathbf{e}_x^0(k+1)^T P_c \mathbf{e}_x^0(k+1) \\ = \mathbf{e}_x^T(k) \Phi^T(u^0(r_I)) P_c \Phi(u^0(r_I)) \mathbf{e}_x(k) \quad (16)$$

for all  $k$ , where  $\Phi(u^0(r_I)) := A_2 + G u^0(r_I)$ . Considering the difference  $J(\mathbf{e}_x(k), u^0(r_I)) - J(\mathbf{e}_x(k-1), u(k-1))$ , it is easy to see that the following inequality:

$$\Phi^T(u^0(r_I)) P_c \Phi(u^0(r_I)) - P_c < 0 \quad (17)$$

ensures that

$$J(\mathbf{e}_x(k), u^0(r)) - J(\mathbf{e}_x(k-1), u(k-1)) = -\mathbf{e}_x^T(k) Q_c \mathbf{e}_x(k) - \rho \tilde{u}^2(k-1) < 0 \quad \forall k \quad (18)$$

where  $Q_c := P_c - \Phi^T(u^0(r_I)) P_c \Phi(u^0(r_I)) (> 0)$ . From the optimality of the MPC (15) with respect to the problem (12), we have

$$J(\mathbf{e}_x(k), u^*(\mathbf{e}_x(k))) \leq J(\mathbf{e}_x(k), u^0(r_I)). \quad (19)$$

Thus, it follows from (18) and (19) that

$$J(\mathbf{e}_x(k), u^*(\mathbf{e}_x(k))) - J(\mathbf{e}_x(k-1), u(k-1)) \leq -\mathbf{e}_x^T(k) Q_c \mathbf{e}_x(k) - \rho \tilde{u}^2(k-1) < 0 \quad \forall k \quad (20)$$

provided that the matrix  $P_c$  meets the inequality (17). Together with this result and the positive definiteness of the cost function  $J(\mathbf{e}_x(k), u(k))$  in terms of  $\mathbf{e}_x(k)$  and  $\tilde{u}(k)$ , it is concluded that

$$\lim_{k \rightarrow \infty} \mathbf{e}_x(k) = \mathbf{0} \quad \forall \mathbf{e}_x(0) \neq \mathbf{0}. \quad (21)$$

This analysis is summarized as Theorem 1.

*Theorem 1:* Suppose that matrix  $P_c$  of the cost function (11) is chosen to be a solution of (17). Then, the proposed MPC (15) ensures the property (21).  $\diamond$

Note that, summing up both sides of the inequality (20) from  $k = 1$  to  $\infty$ , we have

$$\begin{aligned} & J(\mathbf{e}_x(k), u(k)) \\ & \geq \sum_{i=0}^{\infty} \left( \mathbf{e}_x^T(k+1+i) Q_c \mathbf{e}_x(k+1+i) + \rho \tilde{u}^2(k+i) \right). \end{aligned} \quad (22)$$

It implies that the proposed method actually minimizes the upper bound on the infinite horizon cost index in receding horizon manner as it was done in the well known MPC method [37]. It can be shown that matrix  $\Phi(u^0(r_I))$  becomes stable for short enough time. It means that this sampling time ensures the solvability of the inequality (17) in terms of  $P_c$ . Thus, with this sampling time, if matrix  $P_c$  is chosen for the MPC to satisfy (17), the result of Theorem 1 is guaranteed. The inequality (17) can be equivalently rewritten, using the Shur complement [38], as follows:

$$\begin{bmatrix} P_c & P_c \Phi(u^0(r_I)) \\ \Phi^T(u^0(r_I)) P_c & P_c \end{bmatrix} > 0. \quad (23)$$

Note that inequality (23) is affine in terms of  $u^0(r)$ . Thus, it is easy to see that a solution of

$$\begin{aligned} & \begin{bmatrix} P_c & P_c \Phi(D_{\min}) \\ \Phi^T(D_{\min}) P_c & P_c \end{bmatrix} > 0 \\ & \begin{bmatrix} P_c & P_c \Phi(D_{\max}) \\ \Phi^T(D_{\max}) P_c & P_c \end{bmatrix} > 0 \end{aligned} \quad (24)$$

satisfies inequality (23) for any admissible  $r_I$ . Therefore, the result of Theorem 1 is also valid if matrix  $P_c$  is chosen to satisfy the two inequalities in (24). There might exist many solutions to the two inequalities in (24). For example, matrix  $P_c$  can be selected with the minimum trace as long as  $P_c > \gamma I$  for some  $\gamma > 0$ .

#### D. Use of State Constraints

This section describes how state constraints can be handled in the proposed MPC method. Consider state constraints given by

$$\underline{i}_L \leq i_L(k) \leq \bar{i}_L, \quad \underline{v}_c \leq v_c(k) \leq \bar{v}_c \quad \forall k. \quad (25)$$

Then, the optimization problem (12) should be solved under additional constraints that the predicted state  $\mathbf{x}(k+1) = [i_L(k+1) v_c(k+1)]^T$  satisfies the state constraints (25). Based on the state equation (3), the constraint (25) can be applied to the predicted state

$$\mathbf{x}(k+1) = A_2 \mathbf{x}(k) + (B + G \mathbf{x}(k)) u(k) + B_2 \mathbf{v}$$

to yield the following constraints on input  $u(k)$ :

$$\underline{c}_{i_L}(k) \leq u(k) \leq \bar{c}_{i_L}(k) \quad \forall k \quad (26)$$

$$\underline{c}_{v_c}(k) \leq u(k) \leq \bar{c}_{v_c}(k) \quad \forall k \quad (27)$$

where  $\underline{c}_{i_L}(k)$ ,  $\bar{c}_{i_L}(k)$ ,  $\underline{c}_{v_c}(k)$ , and  $\bar{c}_{v_c}(k)$  can be obtained by manipulating the conditions  $\underline{i}_L \leq i_L(k+1) \leq \bar{i}_L$  and  $\underline{v}_c \leq v_c(k+1) \leq \bar{v}_c$ . Including these constraints (26) and (27), the MPC problem (12) can be modified as

$$\min_{u(k) \in [D'_{\min}(k), D'_{\max}(k)]} J(\mathbf{e}_x(k), \mathbf{u}(k)) \quad \forall k \geq 0 \quad (28)$$

where

$$D'_{\min}(k) := \max\{D_{\min}, \underline{c}_{i_L}(k), \underline{c}_{v_c}(k)\}$$

$$D'_{\max}(k) := \min\{D_{\max}, \bar{c}_{i_L}(k), \bar{c}_{v_c}(k)\}.$$

The solution of (28) is obtained through the same way as Section III-B

$$u^*(\mathbf{e}_x(k)) = \begin{cases} u_{uc}^*(\mathbf{e}_x(k)) \text{ (of (14))}, & \text{if } D'_{\min}(k) \leq u_{uc}^*(\mathbf{e}_x(k)) \leq D'_{\max}(k) \\ D'_{\min}(k), & \text{if } u_{uc}^*(\mathbf{e}_x(k)) < D'_{\min}(k) \\ D'_{\max}(k), & \text{if } u_{uc}^*(\mathbf{e}_x(k)) > D'_{\max}(k). \end{cases} \quad (29)$$

Note that the constrained optimization problem (28) is feasible when the set  $[D'_{\min}(k), D'_{\max}(k)] := [D_{\min}, D_{\max}] \cap [\underline{c}_{i_L}(k), \bar{c}_{i_L}(k)] \cap [\underline{c}_{v_c}(k), \bar{c}_{v_c}(k)]$  is not empty.

*Remark 1:* The property of Theorem 1 cannot be applied to MPC (29) since the use of steady-state input  $u^0(r_I)$  does not guarantee that the state at the next time step satisfies the state constraint (25). In order to avoid this problem, consider another type of state constraint defined as

$$\mathbf{e}_x^T(k) P_c \mathbf{e}_x(k) = (\mathbf{x}(k) - \mathbf{x}^0(r_I))^T P_c (\mathbf{x}(k) - \mathbf{x}^0(r_I)) \leq c \quad (30)$$

where  $c$  is the adjustable constant. It is easy to see that the set

$$\Omega(P_c, c) := \{\mathbf{e}_x \mid \mathbf{e}_x^T P_c \mathbf{e}_x \leq c\}$$

is invariant with respect to the steady-state input  $u(k) = u^0(r_I)$  for any  $c > 0$  provided that matrix  $P_c$  of the cost function is chosen to satisfy the inequality (17). Taking the state constraint

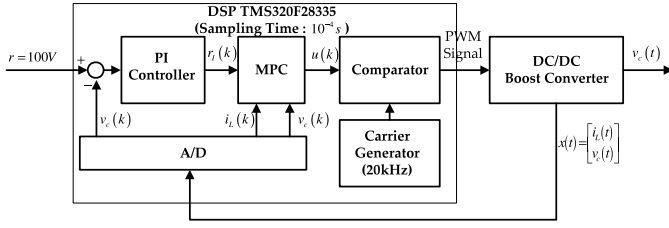


Fig. 3. Hardware configuration.

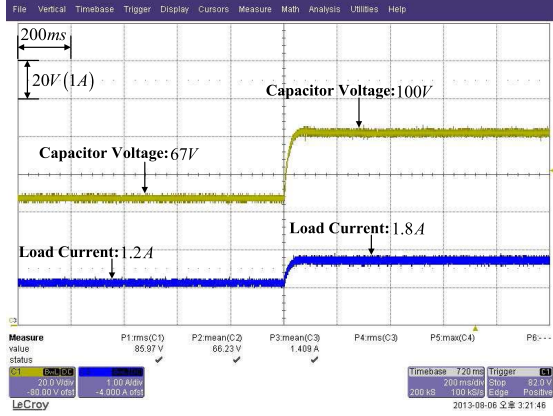


Fig. 4. Voltage tracking performance and corresponding load current behavior with the reference transition from 67 to 100 V.

(30) into account, we modify the optimization problem (12) as follows:

$$\begin{aligned} \min_{u(k) \in [D_{\min}, D_{\max}]} & J(\mathbf{e}_x(k), u(k)) \\ \text{subject to } & \mathbf{e}_x(k+1) \in \Omega(P_c, c^*) \quad \forall k \geq 0 \end{aligned} \quad (31)$$

where the positive constant  $c^*$  is properly chosen by considering allowable state ranges. Note that the constraint  $\mathbf{e}_x(k+1) \in \Omega(P_c, c^*)$  can be written as

$$\begin{aligned} \mathbf{e}_x^T(k+1)P_c\mathbf{e}_x(k+1) &= J(\mathbf{e}_x(k), u(k)) - \rho\tilde{u}^2(k) \\ &= c_2(\mathbf{e}_x(k))u(k)^2 + c_1(\mathbf{e}_x(k))u(k) \\ &\quad + c_0(\mathbf{e}_x(k)) \leq c^* \end{aligned}$$

where  $c_2(\mathbf{e}_x(k)) > 0$ ,  $\forall k$ . Let  $\underline{u}(k)$  and  $\tilde{u}(k)$  be the roots of the equation  $\mathbf{e}_x^T(k+1)P_c\mathbf{e}_x(k+1) = c_2(\mathbf{e}_x(k))u(k)^2 + c_1(\mathbf{e}_x(k))u(k) + c_0(\mathbf{e}_x(k)) = 0$  where  $\underline{u}(k) \leq \tilde{u}(k)$ . Then, the solution of MPC (29) can be used after redefining  $D'_{\min}(k)$  and  $D'_{\max}(k)$  as  $D'_{\min}(k) = \max\{D_{\min}, \underline{u}(k)\}$  and  $D'_{\max}(k) = \min\{D_{\max}, \tilde{u}(k)\}$ , respectively. From the invariance of the set  $\Omega(P_c, c^*)$ , the optimization problem (31) remains feasible for all  $k > 0$  and the property of Theorem holds if the optimization problem (31) is feasible at  $k = 0$ . The state constraint of (30), however, is centered at  $\mathbf{x}^0(r_I)$  and it could be too conservative to cover the region defined as (25).  $\diamond$

#### IV. VOLTAGE CONTROLLER DESIGN IN OUTER LOOP

This section presents a guideline for choosing PI gains of the outer-loop voltage control. To this end, suppose that the inner-loop control system with the MPC is sufficiently fast so

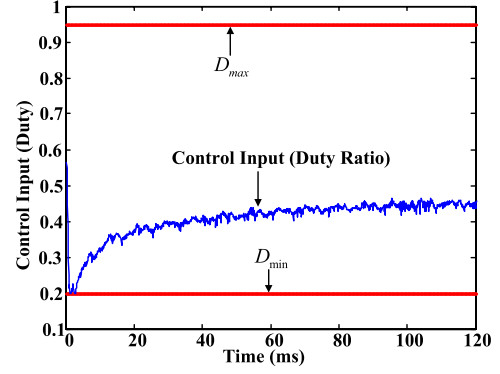
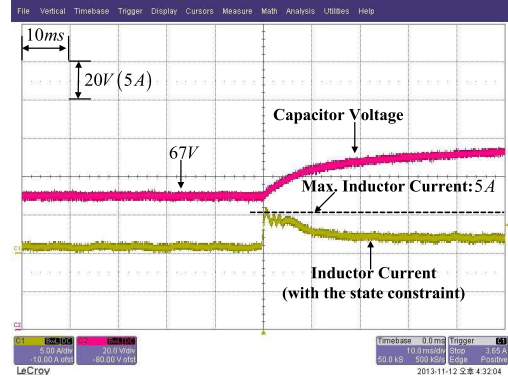


Fig. 5. Behavior of control input after the reference transition over 120 ms.


 Fig. 6. Voltage tracking performance and corresponding load current behavior with the reference  $r = 100$  V (magnified) with the state constraint.

that it can be assumed that

$$i_L(k) \approx r_I(k) \quad (32)$$

where  $r_I(k)$  is a slowly time-varying signal. Since the inner-loop MPC (15) is a deadbeat-type controller, it is reasonable to assume that the inner loop is much faster than the outer loop. In addition, this kind of assumption is also used in [39] and [40]. Let signal  $r_I(k)$  be the output of the outer-loop PI controller as follows:

$$r_I(k) = k_P(r - v_c(k)) + k_I \sum_{j=0}^k (r - v_c(j)) \quad \forall k \quad (33)$$

where  $r$  denotes a reference for  $v_c(k)$  such that there exists an admissible inductor current reference  $r_I$  satisfying  $r = x_2^0(r_I)$ . Then, through algebraic manipulations with the assumption (32), it follows that

$$e_{v_c}(k+2) + \eta_1(k_P, k_I)e_{v_c}(k+1) + \eta_0(k_P)e_{v_c}(k) = 0 \quad \forall k \quad (34)$$

where

$$\begin{aligned} e_{v_c}(k) &:= r - v_c(k) \\ \eta_1(k_P, k_I) &:= \frac{1}{C}(k_P + k_I) + \frac{1}{RC} - 2 \\ \eta_0(k_P) &:= 1 - \frac{1}{C} \left( \frac{1}{R} + k_P \right). \end{aligned}$$

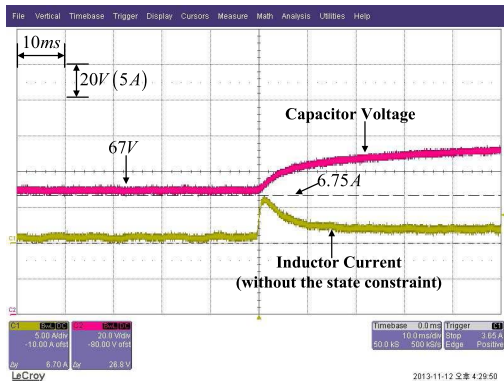


Fig. 7. Voltage tracking performance and corresponding load current behavior with the reference  $r = 100$  V (magnified) without the state constraint.

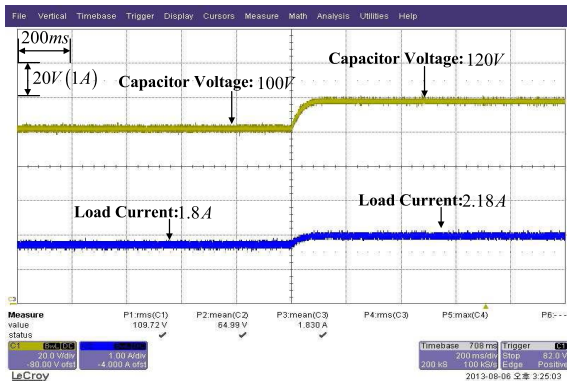


Fig. 8. Voltage tracking performance and corresponding load current behavior with the reference  $r = 120$  V.

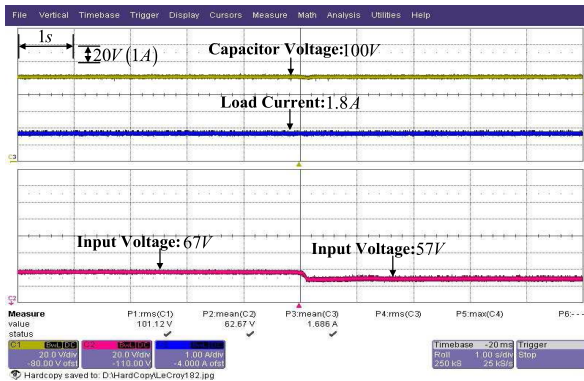


Fig. 9. Voltage regulation performance and corresponding load current under input voltage change.

Since it is possible to arbitrarily assign the pole of the characteristic equation (34) by the PI gains, the capacitor voltage regulation of  $\lim_{k \rightarrow \infty} v_c(k) = r$  can be achieved through the outer loop PI controller. Note that this analysis is justified if the inner-loop control system is sufficiently fast such that signal  $c(k)$  generated by the outer-loop PI controller can be treated as a constant.

## V. EXPERIMENTAL RESULT

In this section, we consider a 3-kW boost converter shown in Fig. 1 in which the switch is the IGBT (IKW50N60T) and

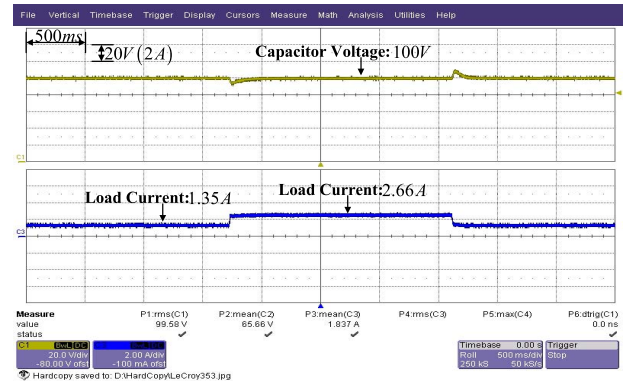


Fig. 10. Voltage regulation performance and corresponding load current under load resistance change from 75 to 37.5  $\Omega$ .

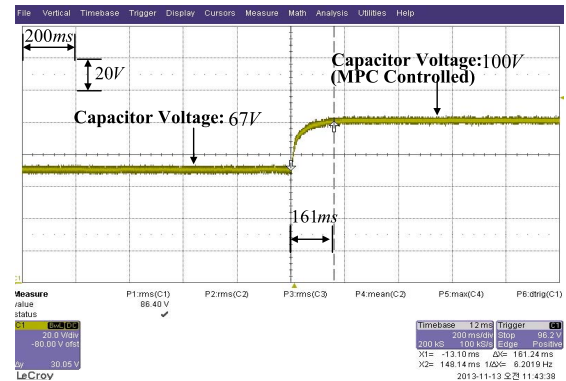


Fig. 11. Tracking performance of the proposed MPC.

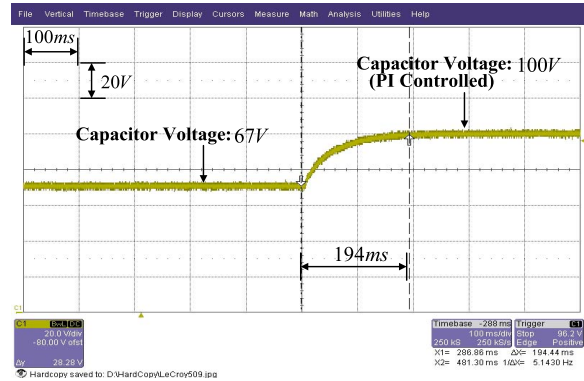


Fig. 12. Tracking performance of the classical cascade PI control scheme.

the parameters are given by

$$R = 50 \Omega, \quad C = 1880 \mu\text{F}, \quad L = 3 \text{ mH} \\ R_{ON} = 0.08 \Omega, \quad v_g = 67 \text{ V}, \quad v_D = 0.67 \text{ V}.$$

For PWM, the switching frequency is chosen as 20 kHz. The MPC algorithm (29) is implemented by using the digital signal processor TMS320F28335 with a sampling time of  $h = 0.1$  ms. The inductor current and capacitor voltage are measured by the CT-type Hall sensor and the PT-type voltage sensor, respectively. The minimum and maximum duty cycles are set to be  $D_{\min} = 0.2$  and  $D_{\max} = 0.95$  so that

$[D_{\min}, D_{\max}]$  is the largest interval contained in the interval  $[0, 1]$ , ensuring the existence of  $P_c$  satisfying inequality (24). If the interval of  $[D_{\min}, D_{\max}]$  were set to be small, the closed-loop performance would be degraded. On the basis of matrices  $\Phi(D_{\min})$  and  $\Phi(D_{\max})$  calculated by these parameters, matrix  $P_c$  satisfying the inequality (24) is chosen as

$$P_c = \begin{bmatrix} 0.0016 & 0 \\ 0 & 0.001 \end{bmatrix}$$

in such a way that  $P_c$  has the minimum trace as long as  $P_c > 0.001I$ . The control weight  $\rho$  of the cost function (11) is set to be 0.01. The admissible ranges of the steady-state control and the capacitor voltage reference with these parameters found to be  $[1.4, 250]$  and the corresponding capacitor voltage range is  $[84, 950]$ . For the outer loop, the PI gains are tuned as

$$k_{\text{out},P} = 0.1 \quad k_{\text{out},I} = 3$$

so that the all poles of the characteristic equation (34) are within the unit circle and the capacitor voltage response is as fast as possible while there is no overshoot. Fig. 3 shows the hardware configuration for this experiment. The following state constraints are used in the design of the proposed MPC:

$$0 \text{ A} \leq i_L(k) \leq 5 \text{ A}, \quad 0 \text{ V} \leq v_c(k) \leq 150 \text{ V} \quad \forall k. \quad (35)$$

Figs. 4 and 5 show that the MPC successfully forces the capacitor voltage to track the reference voltage  $r = 100 \text{ V}$  while satisfying the input constraint when the initial capacitor voltage is  $67 \text{ V}$ .

Fig. 6 magnifies the transition of Fig. 4. Fig. 7 shows that the state constraint is violated when the MPC is designed without the state constraint (35). It can be seen in Fig. 8 that the MPC also provides a satisfactory voltage tracking performance when the reference voltage is changed from 100 to 120 V. The next experiments are carried out to show the regulation performance when the input voltage and the load resistance is changed. Figs. 9 and 10 show that the proposed MPC robustly regulates the capacitor voltage despite the changes of the input voltage (from 67 to 57 V) and load variations (from 75 to 37.5  $\Omega$ ), respectively.

Now, we compare the tracking performances of the proposed MPC scheme with the classical cascade PI control scheme. The outer-loop PI gains are chosen to be same with the MPC, and the inner-loop PI gains are tuned to be  $k_{\text{in},P} = 0.2, k_{\text{in},I} = 0$  so that the capacitor voltage response is as fast as possible, while there is no overshoot. Note that, for fair comparison, the integrator gain of the inner loop is set to be zero since the MPC does not include the integrator. Figs. 11 and 12 show that the proposed MPC considerably enhances the tracking performance as compared with the classical one. It is observed that a higher proportional gain  $k_{\text{in},P} = 0.22$  makes the closed-loop system unstable.

## VI. CONCLUSION

On the basis of the classical cascade voltage control scheme, utilizing a nonlinear dc/dc converter model, an MPC scheme is

proposed for the inner loop with closed-loop stability analysis. The online solution of the MPC is given analytically by minimizing a cost function without the use of numerical methods. Following the classical cascade voltage control scheme, a PI controller is used in the outer loop. Finally, it is observed that the closed-loop performance is considerably enhanced as compared with the classical cascade PI control scheme through the experiments.

## REFERENCES

- [1] S.-K. Kim, J.-S. Kim, and Y. I. Lee, "A model predictive control (MPC) for voltage regulation of a DC/DC converter," in *Proc. Eur. Conf. Power Electron. Appl.*, 2013, pp. 1–9.
- [2] A. I. Pressman, *Switching Power Supply Design*. New York, NY, USA: McGraw-Hill, 1998.
- [3] J. Alvarez-Ramirez, I. Cervantes, G. Espinosa-Perez, P. Maya, and A. Morales, "A stable design of PI control for DC-DC converters with an RHS zero," *IEEE Trans. Circuits Syst. I, Fundam. Theory Appl.*, vol. 48, no. 1, pp. 103–106, Jan. 2001.
- [4] G. P. Alexander, G. Feng, L. Yan-Fei, and C. S. Paresch, "A design method for PI-like fuzzy logic controllers for DC-DC converter," *IEEE Trans. Ind. Electron.*, vol. 54, no. 5, pp. 2688–2696, Oct. 2007.
- [5] W. Stefanutti, P. Mattavelli, S. Saggini, and M. Ghioni, "Autotuning of digitally controlled DC-DC converters based on relay feedback," *IEEE Trans. Power Electron.*, vol. 22, no. 1, pp. 199–207, Jan. 2007.
- [6] H. S. Ramirez, "Nonlinear P-I controller design for switchmode DC-to-DC power converters," *IEEE Trans. Circuits Syst.*, vol. 38, no. 4, pp. 410–417, Apr. 1991.
- [7] S. Bibian and H. Jin, "High performance predictive dead-beat digital controller for DC power supplies," *IEEE Trans. Power Electron.*, vol. 17, no. 3, pp. 420–427, May 2002.
- [8] P. Shanker and J. M. S. Kim, "A new current programming technique using predictive control," in *Proc. 16th Int. Conf. Telecommun. Energy Conf.*, Oct./Nov. 1994, pp. 428–434.
- [9] M. Salimi, "Sliding mode control of the DC-DC fly back converter with zero steady-state error," *J. Basic. Appl. Sci. Res.*, vol. 2, no. 10, pp. 10693–10705, 2012.
- [10] R. Venkataramanan, A. Savanovic, and S. Cuk, "Sliding mode control of DC-DC converters," in *Proc. IECON*, 1985, pp. 252–258.
- [11] H. Sira-Ramirez, "Sliding motions in bilinear switched networks," *IEEE Trans. Circuits Syst.*, vol. 34, no. 8, pp. 913–933, Aug. 1987.
- [12] H. Sira-Ramirez, R. Ortega, R. Perez-Moreno, and M. Garcia-Esteban, "A sliding mode controller-observer for DC-to-DC power converters: A passivity approach," in *Proc. 34th IEEE Conf. Decision Control*, Dec. 1995, pp. 3379–3384.
- [13] J. Mahdavi, A. Emadi, and H. Toliyat, "Application of state space averaging method to sliding mode control of PWM DC/DC converters," in *Proc. Rec. IEEE Ind. Appl. Conf., 32nd IAS Annu. Meeting*, Oct. 1997, pp. 820–827.
- [14] M. Oppenheimer, I. Husain, M. Elbuluk, and J. D. Abreu-Garcia, "Sliding mode control of the cuk converter," in *Proc. 27th Annu. IEEE Power Electron. Spec. Conf.*, Jun. 1996, pp. 1519–1526.
- [15] Y. He and F. Luo, "Sliding-mode control for DC-DC converters with constant switching frequency," in *Proc. Control Theory Appl.*, 2006, pp. 37–45.
- [16] C. Kuo-Hsiang, H. Chun-Fei, L. Chih-Min, L. Tsu-Tian, and L. Chunshien, "Fuzzy-neural sliding-mode control for DC-DC converters using asymmetric Gaussian membership functions," *IEEE Trans. Ind. Electron.*, vol. 54, no. 3, pp. 1528–1536, Jun. 2007.
- [17] L. Jinbo, M. Wenlong, and G. Fanghong, "A new control strategy for improving performance of boost DC/DC converter based on input-output feedback linearization," in *Proc. 8th WCICA*, Jul. 2010, pp. 2439–2444.
- [18] L. Jinbo and M. Wenlong, "A new experimental study of input-output feedback linearization based control of boost type DC/DC converter," in *Proc. IEEE Int. Conf. Ind. Technol.*, Mar. 2010, pp. 685–689.
- [19] T. Hu, "A nonlinear-system approach to analysis and design of power-electronic converters with saturation and bilinear terms," *IEEE Trans. Power Electron.*, vol. 26, no. 2, pp. 399–410, Feb. 2011.

- [20] C. Olalla, I. Queinnec, R. Leyva, and A. E. Aroudi, "Optimal state-feedback control of bilinear DC-DC converters with guaranteed regions of stability," *IEEE Trans. Ind. Electron.*, vol. 59, no. 10, pp. 3868-3880, Oct. 2012.
- [21] C. Olalla, R. Leyva, I. Queinnec, and D. Maksimovic, "Robust gain-scheduled control of switched-mode DC-DC converters," *IEEE Trans. Power Electron.*, vol. 27, no. 6, pp. 3006-3019, Jun. 2012.
- [22] C. Olalla, R. Leyva, A. E. Aroudi, and I. Queinnec, "Robust LQR control for PWM converters: An LMI approach," *IEEE Trans. Ind. Electron.*, vol. 56, no. 7, pp. 2548-2558, Jul. 2009.
- [23] Y. Yao, F. Fassinou, and T. Hu, "Stability and robust regulation of battery-driven boost converter with simple feedback," *IEEE Trans. Power Electron.*, vol. 26, no. 9, pp. 2614-2626, Sep. 2011.
- [24] S. Kouros, P. Cortes, R. Vargas, U. Ammann, and J. Rodriguez, "Model predictive control—A simple and powerful method to control power converters," *IEEE Trans. Ind. Electron.*, vol. 56, no. 6, pp. 1826-1838, Jun. 2009.
- [25] M. Lazar, W. P. M. H. Heemels, B. J. P. Roset, H. Nijmeijer, and P. P. J. van den Bosch, "Input-to-state stabilizing sub-optimal NMPC with an application to DC-DC converters," *Int. J. Robust Nonlinear Control*, vol. 18, no. 8, pp. 890-904, 2008.
- [26] J. Neely, R. DeCarlo, and S. Pekarek, "Real-time model predictive control of the Ćuk converter," in *Proc. IEEE 12th Workshop Control Model. Power Electron.*, Jun. 2010, pp. 1-8.
- [27] M. Lazar and R. D. Keyser, "Non-linear predictive control of a DC-to-DC converter," in *Proc. SPEEDAM*, Capri, Italy, 2004, pp. 1-5.
- [28] A. G. Beccuti, S. Mariethoz, S. Cliquennois, S. Wang, and M. Morari, "Explicit model predictive control of DC-DC switched-mode power supplies with extended Kalman filtering," *IEEE Trans. Ind. Electron.*, vol. 56, no. 6, pp. 1864-1874, Jun. 2009.
- [29] T. Geyer, G. Papafotiou, and M. Morari, "Hybrid model predictive control of the step-down DC-DC converter," *IEEE Trans. Control Syst. Technol.*, vol. 16, no. 6, pp. 1112-1124, Nov. 2008.
- [30] V. Spinu, A. Oliveri, M. Lazar, and M. Storace, "FPGA implementation of optimal and approximate model predictive control for a buck-boost DC-DC converter," in *Proc. IEEE Int. Conf. Control. Appl.*, Oct. 2012, pp. 1417-1423.
- [31] R. De Keyser, "A gentle introduction to model based predictive control," in *Proc. Int. Conf. Control Eng. Signal Process.*, Piura, Peru, 1998, pp. 16-24.
- [32] A. Bemporad, F. Borrelli, and M. Morari, "Model predictive control based on linear programming—The explicit solution," *IEEE Trans. Autom. Control*, vol. 47, no. 12, pp. 1974-1985, Dec. 2002.
- [33] F. Borrelli, *Constrained Optimal Control of Linear and Hybrid Systems*. New York, NY, USA: Springer-Verlag, 2003.
- [34] O. Hegrenas, J. T. Gravdahl, and P. Todel, "Spacecraft attitude control using explicit model predictive control," *Automatica*, vol. 41, no. 12, pp. 2107-2114, 2005.
- [35] R. W. Erickson and D. Maksimovic, *Fundamentals of Power Electronics*, 2nd ed. New York, NY, USA: Springer-Verlag, 2001.
- [36] V. Spinu, N. Athanasopoulos, M. Lazar, and G. Bitsoris, "Stabilization of bilinear power converters by affine state feedback under input and state constraints," *IEEE. Trans. Circuits Syst. II, Exp. Briefs*, vol. 59, no. 8, pp. 520-524, Aug. 2012.
- [37] M. Kothare, V. Balakrishnan, and M. Morari, "Robust constrained model predictive control using linear matrix inequalities," *Automatica*, vol. 32, no. 10, pp. 1361-1379, 1996.
- [38] S. Boyd, L. E. Ghaoui, E. Feron, and V. Balakrishnan, *Linear Matrix Inequalities in System and Control Theory*. Philadelphia, PA, USA: SIAM, 1994.
- [39] T.-S. Lee, "Input-output linearization and zero-dynamics control of three-phase AC/DC voltage-source converters," *IEEE Trans. Power Electron.*, vol. 18, no. 1, pp. 11-22, Jan. 2003.
- [40] T.-S. Lee, "Lagrangian modeling and passivity-based control of three-phase AC/DC voltage-source converters," *IEEE Trans. Ind. Electron.*, vol. 51, no. 4, pp. 892-902, Aug. 2004.